Journal of Building Engineering 67 (2023) 106040

Contents lists available at ScienceDirect

Journal of Building Engineering

journal homepage: www.elsevier.com/locate/jobe

Modelling virtual sensors for real-time indoor comfort control

H. Edtmayer [a,*], D. Brandl [a], T. Mach [a], E. Schlager [b], H. Gursch [b], M. Lugmair [c], C. Hochenauer [a]

[a] Institute of Thermal Engineering, Graz University of Technology, Austria
[b] Know-Center GmbH, Austria
[c] Salzburg University of Applied Sciences, Austria

ARTICLE INFO

Keywords:
Digital twin
Model-based virtual sensors
Coupled real-time building simulation model
Building indoor comfort control

ABSTRACT

Increasing demands on indoor comfort in buildings and urgently needed energy efficiency measures require optimised HVAC systems in buildings. To achieve this, more extensive and accurate input data are required. This is difficult or impossible to accomplish with physical sensors. Virtual sensors, in turn, can provide these data; however, current virtual sensors are either too slow or too inaccurate to do so. The aim of our research was to develop a novel digital-twin workflow providing fast and accurate virtual sensors to solve this problem. To achieve a short calculation time and accurate virtual measurement results, we coupled a fast building energy simulation and an accurate computational fluid dynamics simulation. We used measurement data from a test facility as boundary conditions for the models and managed the coupling workflow with a customised simulation and data management interface. The corresponding simulation results were extracted for the defined virtual sensors and validated with measurement data from the test facility. In summary, the results showed that the total computation time of the coupled simulation was less than 10 min, compared to 20 h of the corresponding CFD models. At the same time, the accuracy of the simulation over five consecutive days was at a mean absolute error of 0.35 K for the indoor air temperature and at 1.2% for the relative humidity. This shows that the novel coupled digital-twin workflow for virtual sensors is fast and accurate enough to optimise HVAC control systems in buildings.

1. Introduction

Due to the increasing demands on thermal comfort as well as the rising temperatures caused by climate change, more and more cooling systems are being installed in buildings. However, some of these systems often cause unpleasant side effects in human perceived thermal comfort such as locally too low temperatures or drafts due to high air velocities. To combat climate change, the additional CO_2e emissions caused by these cooling systems must also be minimised as far as possible. To counter this, a precise control of the room air conditioning system increases the thermal comfort in the building as well as raises its efficiency and thus lowers its energy consumption and CO_2e emissions.

Human perceived thermal comfort is an important aspect in building conditioning but is difficult to quantify objectively. This is due to the fact that the comfort humans perceive is composed of a multitude of influence factors including subjective ones like personal physique, activity, or clothing, and objective physical factors like air temperature, humidity, or airspeed [1]. Capturing the thermal

* Corresponding author. Institute of Thermal Engineering, Graz University of Technology, Inffeldgasse 25b, 8010, Graz, Austria.
E-mail address: hermann.edtmayer@tugraz.at (H. Edtmayer).

https://doi.org/10.1016/j.jobe.2023.106040
Received 23 August 2022; Received in revised form 1 December 2022; Accepted 1 February 2023
Available online 3 February 2023

comfort is an important prerequisite to control and optimise the room climate conditions so that high building energy efficiency and high user comfort can be met at the same time [2]. On the one hand, building users should experience high thermal comfort and should not be disturbed neither by clunky measurement equipment nor unsatisfactory comfort conditions. On the other hand, the building energy efficiency needs to be raised to reduce CO_2e emissions and meet energy reduction targets.

In order to meet these requirements, sophisticated control strategies and thus comprehensive information on the indoor conditions are necessary. Collecting such comprehensive data in busy indoor spaces with physical sensors alone is a virtually impossible task. The necessary sensors would fill the entire room and thus severely hinder the users and the resulting system costs would also be far too high [3]. Furthermore, physical sensors suffer from outliers, failures, drift and offsets [4] and thus have a limited lifetime.

Therefore, attempts are being made to circumvent these problems with the use of virtual sensors [5]. Virtual sensors are part of simulation models and can provide virtual measurement data from simulation results. Whereas physical measurement data is provided by physical sensors and measurement systems in the real physical world. Virtual sensors, also referred to as soft sensors, are used as a substitute for physical sensors due to reasons such as cost, harsh conditions, lacking availability of energy supplies, or practicability [6]. They can provide a variety of measured variables such as temperature, irradiation, flow velocity, humidity or CO_2 concentration. However, there is still a trade-off between accuracy and computation time of model-based virtual sensors when applied in computational fluid dynamics models [7].

The aim of this research work is to model fast and accurate virtual sensors which can capture the required comprehensive information about the actual state of the indoor environment for improved control of the HVAC system in the building. To provide these virtual sensors, we have created a novel model-based digital twin of the real physical building. The digital twin model is comprised of a building energy simulation model (BES) coupled with a computational fluid dynamics model (CFD) of a physical test facility (test box). We connected these models via a custom simulation control data interface (SCDI) built in Matlab. The physical sensors needed are replaced by virtual sensors in the modelled environment of the test facility. We validated the output of the virtual sensors using the comprehensive measurement data of the test facility. Standard measurement data of a building management system combined with standard building boundary condition values (e.g., the overall heat transfer coefficient of walls and windows) are sufficient as input boundary conditions for the simulation models (CFD and BES) of the digital twin. Other standard building boundary conditions such as heat transfer coefficients which are not located in the BMS are applied automatically through the modelling software when building the simulation model (in IDA ICE) or added with low manual effort when building the simulation model (Fluent). If the building is built with state-of-the-art materials, standard values for the material properties can be used for the different models (CFD and BES). Thus, the digital twin can be easily applied to state-of-the-art buildings. The simulation models used in the coupled simulation still have to be built manually. Future research work can improve the workflow to higher degrees of automatization (e.g., BIM to SIM).

Additionally, we optimised the simulation runtime for a possible real-time control of the indoor climate. The SCDI is designed to be connected to the control of the HVAC system of the testbed in order to receive information from both the physical and the virtual sensors. Through this it is possible to develop and run an improved control strategy optimised for the thermal comfort and the efficiency of the building.

1.1. Related work

Digital twins are designed to monitor and operate physical assets in real time. Although the concept first appeared in manufacturing, it can be applied to various domains including building operation [8]. The potential application of digital twins in building operation covers such diverse applications as energy [9], smart grids [10], construction monitoring and project management [11], sustainability assessment [12], urban planning [13], maintenance [14], logistics and facilities management [9]. Similarly, the scale of a Digital Twin can also vary considerably, reaching from an apartment up to complete districts [10].

While machine learning and data analytics are prominently used to create digital twins [8], simulation-based digital twins are also described in the literature [9]. Vering et al. [14] show how a simulation-based digital twin can be used to determine the optimum of energy consumption and total costs for air filter replacements. Zaballos et al. [15] combined wireless sensor networks with building information modelling (BIM) to capture and monitor thermal, visual, acoustic, and air quality comfort. Zaballos et al. also highlight the research need in the domain of digital twins applied to building engineering, especially when it comes to testing and smartness of the digital twin. This is in line with other work pointing out research needs for the potential use of digital twins in optimisation [10], digital twin business models [14] and general hurdles and success factors for future digital twin application in building engineering [9].

Virtual sensors are closely linked with digital twins since virtual sensors can interact with digital twins in two possible ways. Firstly, a virtual sensor can receive its value from a digital twin. Secondly, when a virtual sensor receives data of physical sensors and generates its value by manipulating them. Here the virtual sensor can feed its values to a digital twin. A digital twin is clearly required in the first case but not necessarily in the second case, since the value from the virtual sensor can also be used in applications other than the digital twin [5,6]. In any case, virtual sensors can play an important role for managing the thermal comfort in buildings. Ploennigs et al. [16] use a thermal balancing model to create virtual temperature sensors and thus minimise the need for sensor equipment to control the room temperatures and monitor comfort levels. A similar approach is used by Ran et al. [17] to create fast-responding virtual sensors for water flows used as control input in HVAC system. Various models can be used to create virtual sensors. Alonso et al. [18] compare the suitability of different models for virtual sensors describing the cooling and efficiency of chillers in HVAC systems. While machine learning approaches dominate the virtual sensor work, simulation can also be used [19]. Gálvez et al. [20] use simulation-based virtual sensors to generate data for the training, validation and test of data-driven models to detect degradation of air filters in vehicles. A prominent application for virtual sensors is the estimation of the occupation level in rooms. Since it is often not feasible to directly count people entering or exiting the rooms, other data sources are used like WiFi signals [21], calendar and interaction monitoring [22] or combinations of multiple sources [23].

When creating a digital twin, its different parts, e.g., different simulation models, virtual or real sensor data, etc. need to be coupled together. In general, coupling methods can be divided into the coupling of BES and CFD simulation models and the coupling of simulation models with MS or data management system (DMS). A comprehensive literature review of all possible coupling mechanisms of BES and CFD models is presented by Tian et al. [24]. It presents a wide range of different applications using combinations of coupling methods like internal and external coupling or one-way, two-way, static or dynamic data transfer. Barbason & Reiter [25] present the application of coupling BES and CFD to improve overheating prediction in a two-storey building in Belgium. In the study of Fan and Ito [26] the main objective was to analyse the energy conversion performance of a real office space with the help of a coupled CFD-BES simulation. In addition, the control of HVAC systems can be based on simulation results, so-called model-based control [27]. Du et al. [28] optimise the placement of physical temperature sensors, which are integrated in the HVAC control terminal, on the basis of a coupled BES and CFD simulation. There is little literature available on the coupling between simulation tools and MS/DMS, especially when both BES and CFD simulation tools are involved. This method, also known as hardware-in-the-loop (HIL), is mainly used for laboratory experiments in which simulation models or software create specific, sometimes dynamic, boundary conditions, requirements and loads for the hardware implemented in the loop [29,30].

2. Methods

In this section we detail how we modelled a digital twin of a test facility located at the campus of Graz University of Technology (TU Graz). First, we present the logic developed for coupling the different parts of the digital twin. We then provide details on the test facility which is comprised of two small office rooms. These house an extensive sensor mesh for measuring their thermal behaviour and enabling the analysis of thermal comfort for the indoor environment. Furthermore, we present the BES model built using the building simulation software IDA ICE, plus a detailed CFD model built using ANSYS Fluent. These model components are connected by a custom SCDI we developed in Matlab, which is presented at the end of this section.

2.1. Overview on the coupling procedure

A description and overview on the procedure of the simulation coupling is presented here. Fig. 1 shows a schematic of the components used and described above together with a description of how they are connected in the coupling mechanism.

There are three basic levels in which the components are situated. The data collection level is comprised of the measurement system (MS) and the data management system (DMS). The components of this level collect data from the real-world sensors located at the test boxes as well as from virtual sensors in the simulation tools. The data is collected in different resolution qualities and time spans. The simulation data is collected in two matrices, a BES matrix and a CFD matrix, and stored in the DMS. The data collection level is building the bridge between the real-world environment, the test boxes, and the virtual environment, the software tools in the simulation and data analysis level.

The simulation and data analysis level forms the core of the coupling methodology with the SCDI as central control and connection interface. It collects and transfers needed data from the data collection level to the simulation tools and back to the data storage in the DMS. The SCDI also calculates the relevant boundary condition values for the BES and CFD models based in the measurement data. Furthermore, the SCDI's algorithm calls the simulation tools and starts simulation runs with the appropriate models and boundary conditions. After either CFD and BES simulation runs have finished, respectively, the SCDI is collecting the result data and calculates further result values based on the simulation results. In the end it is transferring all data to the DMS's data storage.

The third level is the building control level. At this time, a deeper investigation on this topic has to be left to future investigations. But basic research and first data transfer tests were done. The building control system (BCS) can be fed with real-time information directly from the MS, BES and CFD via the SCDI. Conversely, it can be connected to the DMS data storage to receive historical data also.

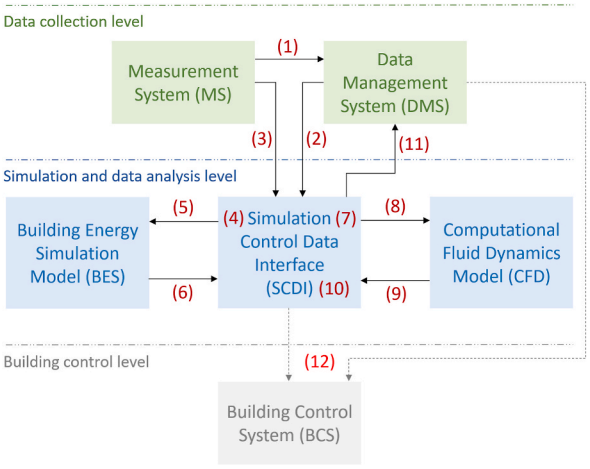

Fig. 1. Schematic of the coupled simulation model of the test boxes at Graz, University of Technology.

Fig. 1 also shows the individual steps of the methodology in hierarchical order of the coupling procedure. Which are.

(1) Measurement data transfer from MS to DMS (45 parameters, mean values, historical)
(2) Measurement data transfer from DMS to SCDI (8 parameters, mean values, historical)
(3) Measurement data transfer from MS to SCDI (8 parameters, high resolution values, real-time)
(4) Preparation for the BES simulation and BES iteration loop
(5) Data transfer from SCDI to BES (8 parameters from (2) or (3))
(6) Data transfer from BES to SCDI (21 parameters)
(7) Preparation for the CFD simulation and CFD iteration loop
(8) Data transfer from SCDI to CFD (21 parameters from BES + 8 parameters from MS)
(9) Data transfer from CFD to SCDI (42 parameters)
(10) Data post-processing for thermal comfort ratings according to Fanger [31].
(11) Data transfer from the SCDI to the DMS (42 + 32 = 74 parameters)
(12) Orders to the BCS

2.2. Test facility at Graz University of Technology

The test facility used in the presented research work is comprised of two outdoor test boxes at Graz University of Technology (shown in Fig. 2), which are located at the Campus Inffeld in Graz, Austria (47.057 North 15.456 East). The energy provision system and the central PLC (programmable logic controller) for the test bed is placed inside a container next to the test boxes.

The test facility was developed in a previous project (MPC-Boxes [32]) to investigate a model predictive control (MPC) strategy for heating and cooling and to compare it to a conventional control system [33].

The test boxes with the facade containing the windows and photovoltaics are oriented to the south. The two boxes are symmetrical and positioned side by side. Each box has the dimensions of $3.2 \times 4.2 \times 2.3$ m. In the north wall a door with a window is integrated. The window as well as the door are built of a polystyrene frame and double glazing. Both test boxes are equipped with an air-handling unit with integrated electric heating coil (1-fold air exchange rate of 30 m^3/h). Test box east is also equipped with a fan coil AC unit to investigate the cooling effect in comparison with the uncooled test box west. A "thermal dummy", an ideal heat and radiation emitter containing of an electric heated metal barrel painted in black is simulating the sum of internal thermal gains of two persons and appropriate computer equipment. This reflects a small office room with a thermal load of 300 W. Both the ventilation system as well as the "thermal dummy" are active from Monday to Friday between 8:00 and 16:00 o'clock while the heating and cooling system is always on. Test box east is conditioned with a decentralized, energy autarky heating and cooling device, which was developed in the previous project "Coolskin" [34]. A photovoltaic plant installed at the south facade of both test boxes provides electricity for operating the air source heat pump system. Results from this research project are published in the article of Bröthaler et al. [35].

The test boxes are equipped with a comprehensive measurement system (MS). The MS contains about 100 measurement sensors with a sampling interval of 1 min. They measure air and wall temperatures as well as humidity at different positions at the interior spaces, walls, ceiling and floor. Table 1 shows the measuring range and measurement uncertainty of the used sensors for temperature and relative humidity.

About half of these measurement points are relevant for the present study and are therefore transferred to the DMS data management system. The data is sent to the DMS as a batch once per day and persistently stored to create long-term time series data. The parameters required for real-time simulation are imported directly from the MS into the SCDI.

The DMS is the central data exchange system in this investigation collecting all relevant monitored and calculated data. Historical data can be taken from the data storage in order to perform simulations used for the model validation. The DMS storage contains data from 2018 to 2021 and is comprised of four main components. The two central components are the time series database InfluxDB and the document storage ArangoDB. While InfluxDB stores the measurement data, ArangoDB holds meta data including measurement unit, location and description information. The two other components are the so-called Bridge and the WebService. Incoming data from sensors, controllers and simulations is collected by the Bridge, reorganised to fit the data model and stored in InfluxDB and ArangoDB, respectively. The WebService provides a web-based human user interface and an interface for the BES and CFD to query

Fig. 2. Test facility at the TU Graz, Campus Inffeldgasse.

Table 1
Properties of the measuring sensors used in the MS.

Measurand	Type	Class	Range	maximum deviation $\delta T(T)$
Temperature	Thermocouple Type T	1	−40 °C … +125 °C	±0,5 K + 0,004 • $\|T\|$
Temperature	Resistance temperature sensor	A	−40 °C … +500 °C	±0,15 K + 0,0017 • $\|T\|$
Operative temperature	Resistance temperature sensor	B	−30 °C … +70 °C	±0,2 K + 0,002 • $\|T\|$
Humidity	Capacitive humidity sensor	–	−10% … 90%	±2%

data. Bridge and WebService hide the fact that the data and metadata is stored separately in InfluxDB and ArangoDB by providing common input and output interfaces.

2.3. Building energy simulation model

The building energy simulation (BES) model presented in this paper is developed using the building energy simulation platform IDA ICE. The test boxes are modelled with inputs about dimensions, construction materials and map orientation. The appropriate thickness and thermal properties of the layer materials of walls, floor and ceiling are used. Also, the size, positioning and materials of windows and doors are implemented. The model additionally contains all the shading relevant objects like building integrated photovoltaic modules (BIPV) and the supply container. The fan coil unit in test box east is considered for room air conditioning and implemented in the model. Furthermore, the ventilation system in the BES model is designed to be switched on and off with the help of the SCDI.

The weather profile used in the model is the in IDA ICE provided data for the location Graz-Thalerhof-Flug_112400 (ASHRAE 2013) in the corresponding simulation period 2017 and 2018 [36]. For the wind profile the exposure type ‘default urban’ is used as there are more buildings in the surrounding area of the test boxes. The infiltration rate of the model was set by results of a blower door test according to EN13829. According to this data a wind-driven-flow model with an air tightness of 1.51 ACH (air changes hour) at 50 Pa pressure difference was used. The thermal bridges were calculated for walls, outside corners, ceiling grid, ground and windows. This resulted in a reduction of the overall U-value of the envelope area of 0.088247 W/m^{2}K and was implemented in the model.

For the climate boundary conditions, measurement data was inserted into the model via a climate data file. On-site measurement of outdoor climate conditions at the test boxes was used as boundary conditions in the simulation. The parameters used in the climate file were dry-bulb temperature, relative humidity of air, direct radiation, diffuse radiation on horizontal surface, wind speed (x-component and y-component) and cloudiness.

The BES model schematic is presented in Fig. 3. The ventilation model is framed in green, the plant model in red, the zone model of test box east in blue and of test box west in yellow. Both zone models are connected to the plant model as energy source for thermal conditioning. Both are also connected to the ventilation model for modelling the air exchange. The zone model of the test box east is

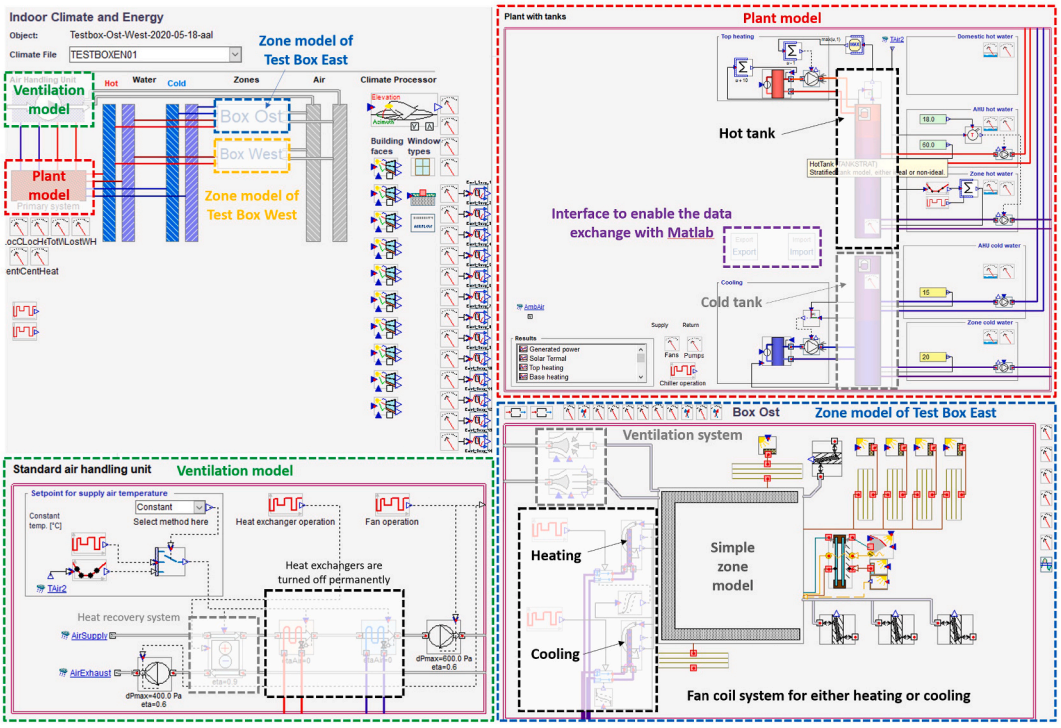

Fig. 3. Snapshot of the BES model schematics.

equipped with one fan coil system for heating and one for cooling. The thermal conditioning is turned off for test box west, only the ventilation model is turned on to account for the absence of the fan coil unit.

The BES model contains one virtual sensor per text box representing the behaviour of the interior average air volume. The following values from the virtual sensors are sent via the Matlab interface to the DMS.

- Air temperature (°C)
- Operative temperature (°C)
- Fanger's comfort indices Predictive Mean Vote (PMV) (−) and Predicted Percentage of Dissatisfied (PPD) (%) [31].
- Relative humidity (%)
- Heat (W) from walls, equipment, occupants, heating/cooling, windows, air flows and solar radiation
- Ventilation mass flow rate (kg/s), supply and return temperature (°C)
- Direct and diffusive solar radiation (W/m^2), exterior temperature (°C) and humidity (%)

2.4. Computational fluid dynamics simulation models

The software tool ANSYS is used for modelling, meshing, simulation and post-processing of the CFD simulation process. The simulation is performed with the software Fluent ANSYS 19.2. The detailed mathematical description of the below-named model parameters and equations can be found in the ANSYS Theory/User Guide [37]. A "pressure-based" type of solver is used for all simulations, the "gravity force" is activated together with the "energy equation". The fluid involved is set as "incompressible ideal gas" to allow the influence of thermal buoyancy effects leading to natural convection. For the description of the flow characteristic the k-model is the most suitable model approach. This is confirmed by a number of varied studies e. g., Refs. [38–40]. The "standard wall function" is used in order to avoid an excessively large number of cells in the model, the additional option of including "full buoyancy effects" is activated. The less time-consuming "S2S" radiation model is used while the impact of solar radiation is considered with the help of the solar calculator embedded in the Fluent software using a simple solar load model. For the comparison between simulation results and measured data an "implicit transient" solving algorithm is used.

The simulation model is also equipped with the "species transport" model allowing the composition of different fluids in the simulation and an interaction between them. In this case the fluid consists of nitrogen (N_2), oxygen (O_2) and water vapour (H_2O). If necessary, the fluid mixture can be extended with carbon dioxide (CO_2). Then, in combination with the "particle tracking" model embedded in the Fluent software, the detailed carbon dioxide concentration can be calculated.

The CFD models require the enclosing temperatures (or heat fluxes), the internal thermal gains (occupants, solar radiation, heating/cooling system, computer, screens, etc.), ventilation in- and outlets (opened window, fan coil, leaks, etc.), water vapour sources and alternatively carbon dioxide sources as its boundary conditions. To reduce the calculation duration, the enclosing walls of the room are defined as a virtual layer in accordance with the material data of the test boxes.

A three-dimensional view of the simulation model created for test box east with an illustration of the surface mesh cells as well as a view inside the interior is presented in Fig. 4. Generally, both test box models are similar (symmetric) except for the fan coil inlets and outlets which do not exist in test box west. The mesh of test box west contains 0.76 million cells, test box east has many more cells with 2.37 million due to the cell refinement of the region around the fan coil inlet. The model contains the whole interior air space; the walls and windows etc. are all composed as virtual layers with the input of the material properties (specific heat capacity, thermal conductivity, density) and the layer thickness. The measured exterior temperature is used as the exterior boundary together with a heat transfer coefficient of 25 W/m^{2}K. The construction of the south facade-integrated heat pump system is not considered in the CFD model because the impact on the heat transfer between interior and exterior can be neglected. The solar radiation can be set as a boundary condition in the form of a surface heat flux, which is determined cell-wise with the in the Fluent software integrated "solar calculator".

A mass flow inlet is defined for the fan coil as well as for the ventilation system. During the simulation the volume flow rate of both the fan coil (264 m^3/h) and the ventilation system (30 m^3/h) are set as constant. While the measured exterior temperature is set as inlet temperature for the ventilation system, an averaged air inlet temperature for each cooling period is set as boundary condition for the fan coil cooling device.

In order to cover all possible operating modes in the CFD simulation, six different CFD models are provided for the coupling and the

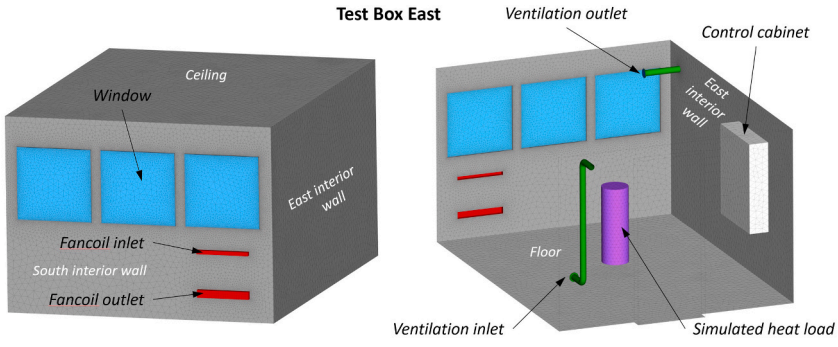

Fig. 4. CFD mesh of the test box east at TU Graz, Inffeldgasse campus.

SCDI decides which one is used at any time. Two different CFD models are provided for test box west, one has an active and the other one has an inactive ventilation. Four different CFD models have to be provided for test box west due to the integrated fan coil unit. This results in four different possible fluid flow states where the ventilation and the fan coil are either on or off. Despite the fact that one model per test box would suffice in theory, there are two reasons for the CFD model subdivision. Firstly, to avoid complications by automatically changing the boundary type from a mass-flow-inlet and pressure-outlet to a standard wall through the SCDI. Secondly, to optimise the number of cells in the model and thus shorten the duration of the CFD simulation. The smallest model, test box west ventilation off, contains about 200,000 cells. The largest model, test box east ventilation on and fan coil on, contains about 1,620,000 cells.

2.4.1. *Virtual sensors in the CFD model*

The virtual sensors defined in the CFD model are illustrated in Fig. 5. In this figure, only the defined virtual sensors of test box east are shown, since the same number and the same position of sensors have been defined in test box west. In the top figure a 3D view of the CFD model with a view into the interior of the room is shown. The contours of the surface temperature are plotted on the surfaces of the room. The flow vectors of the air flow velocity of the fluid dynamics simulation are also shown additionally. The fan coil and ventilation system fans create a clear flow from their outlets towards the centre of the room. A strong flow can also be seen around the ventilation outlet. Furthermore, the internal thermal gains (thermal dummy) generate a small natural convection flow from the centre of the room towards the ceiling. The four virtual sensors used in the investigation are depicted in white spheres. The sensors are placed at a distance of 1.25 m from the floor and in a circle with an 0.8 m diameter around the internal gains source. This can also be seen in the bottom left and in the right figure where the top and the side view of the CFD model are shown, respectively.

The small image on the top right in Fig. 5 shows a view into the real test box east interior towards the south wall, with the thermal gain dummy as black barrel standing upright in the middle of the room and the globe sensors hanging from the ceiling around it. The "XX" in the sensor ID is to be replaced by a parameter similar to air temperature (T-air), humidity (Hum) and the operative temperature (T-op). The "E" stands for test box east and the "N" or "S" stand for sensor position north or south. The transfer of data from the CFD simulation to the interface takes place in the form of text files.

The following values are extracted for each virtual sensor.

- Air temperature, (°C)
- Air flow velocity, (m/s)
- Relative humidity, (%)
- Turbulence intensity, (%)

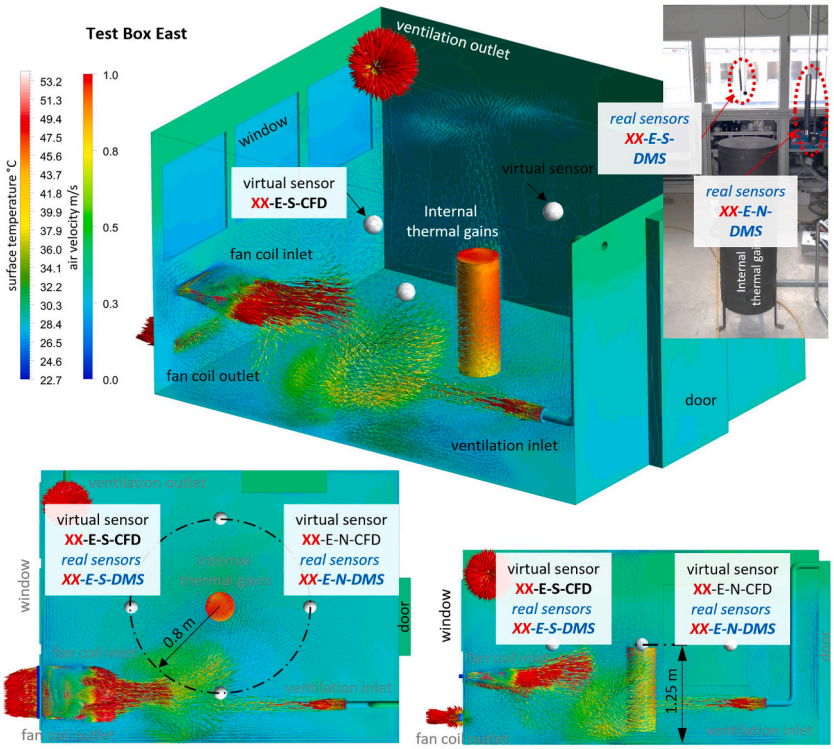

Fig. 5. Surface temperature contours and flow velocity vectors of test box east with the defined virtual sensors depicted as spheres; top big figure: 3D view with view into the interior; bottom left: top view of the room; bottom right: side view of the room; top right: view into the real test box interior towards the south wall, with thermal gain dummy and the real humidity, temperature and globe sensors.

In addition, the overall value for each test box of.

- Maximum air temperature, (°C)
- Minimum air temperature, (°C)
- Maximum flow velocity, (m/s)
- Maximum relative humidity, (%)
- Average surface temperature of the room enclosure surfaces, (°C)

are extracted from the CFD simulation results. These are in total 42 parameters per simulated time step, which are transferred from the CFD simulation to the SCDI interface. The results from the CFD simulation are then processed in the SCDI interface and the following comfort parameters are determined for each virtual sensor.

- PMV, (−)
- PPD, (%)
- Draught rate, (%)
- Operative temperature, (°C)

2.5. Simulation control data interface

To collect the measurement data and to manage the entire simulation process, a simulation data interface (SCDI) was developed using the software Matlab (version R2015b, 32 bit). Two different scripts serve as SCDI for producing either the actual interior thermal conditions for both test boxes or to calculate time series describing historical measurement data. Air temperature, solar radiation and humidity are part of the boundary conditions of the BES and are set by the SCDI. To calculate the exterior air temperature, solar radiation and humidity the values of four exterior surface temperature sensors and two interior sensors are used.

- **Exterior air temperature:** The exterior air temperature is determined by the arithmetic mean value of the two exterior surface temperature sensors mounted on the fully shaded north walls.
- **Exterior humidity:** The exterior humidity is calculated based on the exterior air temperature, the interior air temperature and the interior humidity. The interior humidity is multiplied with the ratio of the interior and exterior saturation vapour pressure. The interior and exterior saturation vapour pressure is calculated using the Magnus equation, see eq. (1).

$$p_s = 611.2 * \exp\left(\frac{17.62 * T}{243.12 * T}\right) \tag{1}$$

- **Solar radiation:** The solar radiation is calculated with the help of two exterior surface temperature sensors per box. One of these two sensors per box is positioned at the roof of the test box and measures the temperature of a horizontal black surface fully exposed to the sun. The second sensor is installed at the vertical north oriented and fully shaded wall of the test box. Under consideration of the convective thermal losses, the global horizontal solar radiation is calculated with the help of the Stefan-Boltzmann equation. Finally, the solar radiation is divided into direct and diffuse radiation in a ratio of 3:1. The solar radiation calculation was validated with pyranometer data from a nearby professional weather station run by the Austrian weather service ZAMG [41].

The wind speed is calculated by the IDA ICE model using the available climate measurement data (here Graz Thalerhof in 2017 and 2018) in combination with the settings for the wind profile of the respective site (here default urban). The atmospheric pressure in all BES and CFD simulations is kept constant at a value of 101325 Pa. The influence of pressure differences on the simulation results is estimated to be negligible. After the boundary condition values are calculated the SCDI starts the BES simulation. When the BES simulation is completed all the results are handed over to the SCDI in form of data arrays to provide the requested boundary conditions of the CFD model. They are stored in the BES result matrix produced during the BES iteration loop.

After the BES is completed the SCDI prepares the CFD model. This can be set to either a single simulation run, describing on moment in time, or to a defined simulation describing a time series. In any case, the SCDI selects the correct CFD model, starts the CFD software via a batch file and gives the commands to set up the simulation correctly. The CFD simulation provides the requested simulation results to the SCDI for the final data processing. This exchange is realized by different text files, so called Journal Files, containing the commands which are read and executed line by line in the CFD software.

The CFD models need the same 8 boundary conditions parameters from the MS and the DMS as the BES. Additionally, the CFD model uses 21 parameters which are calculated by the BES simulation. These parameters are either used to be set directly or for the determination of the remaining required boundary conditions. The boundary conditions for the CFD simulation are.

- **Surface heat fluxes:** The six main interior surfaces, the floor, ceiling, north, east, south and west wall of the CFD model receive the heat flux from the BES results matrix.
- **Indoor air temperature:** The indoor air temperature determined by the BES model is used as a boundary condition and for initialization of the start conditions in the CFD model.
- **Ventilation mass-flow rate:** The mass flow rates of both test boxes are exported from the BES results matrix and are set as boundary conditions in the CFD simulation.

- **Mass fractions of substances in the air:** The mass fractions for water vapour, oxygen, nitrogen and carbon dioxide of the air mixture are calculated with the help of parameters from the DMS and MS. They are set as boundary conditions at the ventilation inlet and for the initialization of the interior air zones.
- **Exterior heat transfer coefficient:** A constant heat transfer coefficient and the exterior temperature are used as boundary conditions at the window panes.
- **Internal thermal gains:** The internal thermal gains are turned on and off according to the BES result matrix.
- **Fan coil parameter:** The mass flow rate and the inlet temperature for the fan coil installed in test box east are also content of the BES result matrix.

After the CFD simulation for a single time step is finished all requested virtual sensor data are transferred to the SCDI and the thermal indoor comfort is determined. Therefore, sub programs in the SCDI calculate the thermal indoor comfort ratings PMV, PPD and Draught Rate (DR) for the virtual sensors defined in the CFD models.

Before starting the CFD simulation for the next time step, all requested results, like the virtual sensor data, are added to a CFD result matrix. The automatic transfer of the data to the DMS is not implemented in the current state of the SCDI but it will be possible to implement it in future. Example time series of the virtual sensor data were implemented in the DMS to test this data flow. Additionally, it is also possible to run only the BES iteration loop without any CFD simulation, if there is a demand to analyse the impact of parameters which are only relevant for the BES model.

3. Results & discussion

With the digital twin's workflow in place and ready to go, we validated the quality of the coupled simulation model based on the measurement data of the test facility. First, we calculated individual time points that show certain climate characteristics such as low or high temperatures or high solar radiation. In a second step we calculated a time series of 5 consecutive days for the virtual sensors with a simulation timestep of 10 min. Subsequently, we compared these results to the measurement data. One time step of the HVAC controls measuring system used in the test boxes described here is 15 min. Thus, the control receives new and updated data every 15 min and uses this data to control the HVAC system. If the simulation results of the virtual sensors are available within this timespan, they can be used by the HVAC control system in the same way as the measurement data of the real, physical sensors. The outcomes show that in the coupled simulation the runtime for one virtual timestep of the HVAC control system could be reduced from around 20 h to less than 10 min. Therefore, the results of our coupled simulation can be used in the HVAC control system. At the same time, amongst others, the accuracy of the simulated room air temperature over 5 consecutive days lies at a mean absolute error of 0.4 K. These outcomes demonstrate that our novel design of the virtual sensors is fast and accurate enough to implement them into the control of HVAC systems and thus improve the indoor comfort and efficiency of buildings.

Table 2
Deviation between simulated and measured values of 9 different time points during the observed time series from 1st of Mai to July 31, 2020; deviations depicted in colours, bars and numbers; green low, red and magenta high.

			lowest ext. T	lowest ext. T	lowest ext. T	highest rad	highest rad	highest rad	highest ext. T	highest ext. T	highest ext. T
Date			06.05.2020	07.05.2020	31.05.2020	02.06.2020	13.06.2020	22.06.2020	28.06.2020	10.07.2020	28.07.2020
Time			04:00	04:00	04:00	12:00	12:00	12:00	14:00	14:00	14:00
T ext.		°C	5.7	6.1	7.9	23.9	27.8	25.2	29.8	30.4	32.2
I Sol.		W/m²	0	0	0	981	942	983	756	872	831
Box West	Hum-N	%	-0.1	0.0	0.2	0.4	4.7	0.7	3.3	1.3	0.6
	Hum-S	%	-1.5	-0.8	-0.7	0.3	3.7	0.4	2.7	-0.7	-0.4
	T-air-N	°C	-0.1	0.0	-0.2	-0.4	-1.8	-0.5	-1.3	-0.6	-0.3
	T-air-S	°C	0.0	0.0	-0.1	-0.3	-1.9	-0.6	-1.6	-0.2	-0.6
	T-op-N	°C	0.3	0.3	0.1	-0.6	-2.2	-0.6	-1.7	-0.8	-0.6
	T-op-S	°C	0.4	0.4	0.3	-0.1	-2.1	-0.1	-1.7	-0.1	-0.5
Box East	Hum-N	%	0.3	0.3	0.2	1.2	5.0	2.0	3.6	-1.2	2.5
	Hum-S	%	0.1	1.1	0.9	2.5	4.9	1.5	2.8	-2.0	3.7
	T-air-N	°C	-0.2	-0.2	-0.2	-0.8	-1.9	-1.1	-1.0	0.3	-0.9
	T-air-S	°C	-0.1	-0.1	-0.1	-0.6	-1.7	-0.2	-0.9	0.4	-1.4
	T-op-N	°C	0.1	0.1	0.1	-0.9	-1.8	-0.4	-0.7	0.4	-0.6
	T-op-S	°C	0.4	0.4	0.4	-0.5	-1.6	0.2	-0.7	0.4	-0.8

3.1. Validation of the coupled simulation workflow

3.1.1. Calculation of single time points

In the first step of the validation, we analysed nine single time points at specific dates between 1st of Mai and July 31, 2020. Three distinctive states of the outdoor conditions within the test period are used for this. Firstly, the lowest outdoor air temperature (6th, 7th and 31st of Mai at 04:00 o'clock), followed by the strongest global solar radiation (2nd, 13th and 22nd of June at 12:00 o'clock) and finally the highest outdoor air temperature (28th of June, 10th and 28th of July at 14:00 o'clock).

In the test, the coupled simulation procedure is carried out as described above for the respective day from 0 h to 24 h. The respective data (temperature, radiation, humidity, etc.) from the measurement data recording are used as start boundary conditions. The sensors considered are those for each test box located north and south of the internal thermal gain (see also Fig. 5). The deviations are calculated from simulated minus measured values of the sensors and are summarised in Table 2.

The deviation of the relative humidity of each sensor is coloured from green (low, 0 K) to magenta (high, ±5 K). And the deviation of the room air temperature and the operative room temperature are coloured from green (low, 0 K) to red (high, ±2.2 K). Additionally, the deviations are also depicted in bars and in numbers. According to Table 1, the minimum measurement uncertainty of the temperature sensors is at ±0,15 K. With the additional error of the measuring chain the measurement uncertainty of the temperature measurement is at ±0,3 K. For the relative humidity the measurement uncertainty of the sensor including the measuring chain is at ±2%. Therefore, all results residing in the range of the measurement uncertainty can be seen as very satisfying. Especially for times with low ambient temperatures and no solar radiation the model fits very well to the measured values. At the same time, two days in test box west (13th and 28th of June) and three days in test box east (13th and 28th of June, 28th of July) stand out where the deviation between the model and the measurement is high. The three days with lowest external temperature (6th, 7th and 31st of May) show very satisfying results. The maximum deviation of the indoor air temperature is −0.2 K. The operative indoor temperature, which combines radiation and convection heat transfer, also shows a very small deviation of max. 0.4 K. With a deviation of max. −1.5% the simulation result of the indoor humidity is also very close to measured value in the test box. The day with maximum deviations is the 13th of June at 12:00 noon with a global radiation of 942 W/m^2 and an outdoor temperature of 27.8 °C. The indoor air temperature shows a deviation of −1.9 K and the operative indoor temperature −2.2 K. The relative humidity shows a deviation of 5%.

In the simulation model, the calculated room air temperature is an input variable for the calculation of the operative temperature and the relative humidity. A deviation in the room air temperature thus affects both the operative temperature and the relative humidity results. As a result, the deviation of all values for this time point are influenced.

Additionally, we took a closer look at the measured values to double check for errors. There is measurement data from a nearby

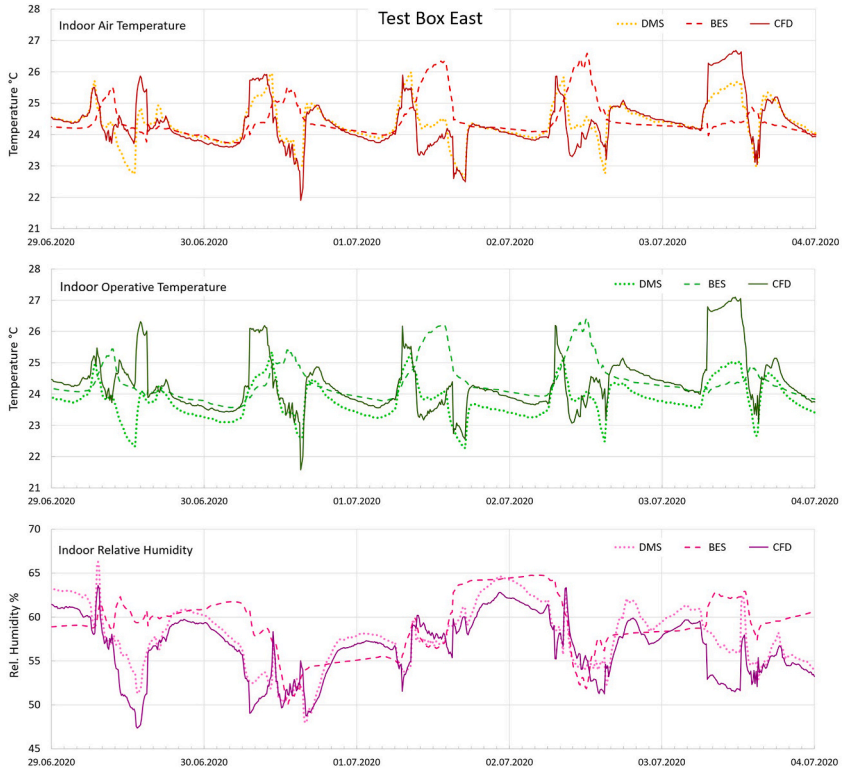

Fig. 6. test box east; Comparison between measurement data from the DMS and simulation results from the BES and the virtual sensor (CFD) from 29.06. to 04.07.2020; top: indoor air temperature, middle: indoor operative temperature, bottom: indoor relative humidity; dotted line: measurement data from DMS, dashed line: simulation data from BES; solid line: simulation data from the virtual sensor (CFD).

meteorological weather station run by the Austrian Central Institute for Meteorology and Geodynamics (ZAMG) available [41]. The measurements of the outdoor temperature for the two test boxes show a clear and repetitive deviation from the ZAMG data. This is especially the case in times with a high level of direct solar radiation (13th and 28th of June). This indicates that the outdoor temperature sensor is affected by reflections of direct solar radiation and is therefore giving readings that are too high. Since the measured outdoor temperature and the resulting relative humidity of the outdoor air are input variables for the building simulation model, deviations in the simulation results also follow from this. We also realized that the 13th of June was a Saturday and the 28th of June a Sunday. On weekends, the thermal dummy and the ventilation system in the test boxes are switched off. At this stage of the experimental tests, we had not yet implemented the weekends in the simulation model and thus the wrong simulation model was used. This contributes to the observed deviations on these two days. In addition, we found that the cooling system in test box east had an error on the 21st of July and was not functional on the 28th of July. The simulation model used thus did not match the real condition of test box east and also contributed to the deviations.

3.1.2. Calculation of time series

In the second step of the model validation, we used the coupled simulation to calculate a time series for the virtual sensors of the test boxes (see also Fig. 5) from 29th of June until July 4, 2020. The simulation time step was set to 10 min, so that the results represent a snapshot of the indoor situation at 10-min intervals. We then compared the results again with the measured values over the same period of time.

Fig. 6 shows the comparison for the test box east. The diagrams depict the comparison between the measured values stored in the DMS, the simulated values of the BES and the final simulation values of the virtual sensors (CFD). Values from the DMS are drawn in dotted lines, BES in dashed lines and CFD in solid lines. The top graph shows the indoor air temperature (red), the middle graph shows the indoor operative temperature (green), and the lower graph shows the indoor relative humidity (magenta).

In general, the virtual sensors show very solid results. Both those sections with good correlation and some sections with an average correlation can be observed. In the timespan from about 16:00 h in the evening to about 8:00 in the morning on each day, the output of the virtual sensors fit very well to the measurement data. During these times, the influences of solar radiation and the outside air temperature are low. On days with high solar radiation levels, i.e., around 900 W/m^2, and a simultaneously high proportion of direct solar radiation (01.07. & 02.07.) the BES model predicts indoor air temperature values that are too high. This results from the problem of the incorrect outdoor temperature measurements described previously and thus of surface heat fluxes from outside into the test boxes that are calculated too high. At times with medium solar radiation, i.e., around 500 W/m^2, and a high share of diffuse solar radiation (03.07. 08:00 to 17:00) the BES model predicts values that are too low. In the boundary conditions assumptions, the ratio of direct to diffuse radiation was set to 3:1. In times with a high proportion of diffuse radiation, this leads to an underestimation of the surface heat flux through those walls that are not directly oriented towards the sun. As a result, the room air temperatures are calculated too low.

In times when the ventilation system is switched on and off the CFD model is changed from the simple model without airflow to the model with ventilation air flow. The model change can be clearly seen in a sharp jump of the indoor air temperature curve at the corresponding times of the day. After a steep rise in the morning, the model changes, which also corresponds very well with the measured values. Subsequently, the simulated indoor air temperature at some time points no longer corresponds optimally to the measured data. Hence, it can be concluded that the air exchange rate in the simulation model with ventilation mass flow was not correctly estimated. The indoor operative temperature profiles show a fairly similar behaviour to the indoor air temperature profiles. Since the indoor air temperature and the indoor operative temperature are directly connected, the behaviour of the models described above is also reflected in the course of the indoor operative temperature. The same applies to the indoor relative humidity, but here the CFD model shows better results than the BES model in most cases.

In addition, the improvement from BES to CFD results is clearly visible. With a more complex air flow situation, the advantages of the CFD model are apparent. There are still sections with a higher deviation, like on 3rd of July between 07:00 h and 12:00 noon. Here the CFD model with activated ventilation system but deactivated air conditioning is used. In contrast, the model with active ventilation and air conditioning systems produces very satisfying results. This was the case for example on 30th of June from 10:30 until 15:00 h. At times when only the air conditioning is on but the ventilation system is off the results are also very good. This can be seen on 1st of July between 14:00 and 17:00. In these cases, the BES model is clearly at a disadvantage and shows considerable deviations from the measured values.

Table 3
Statistical analysis of the calculated time series for both test boxes and two sensors of each test box (north and south); maximum absolute error, mean absolute error and root mean squared error for the deviations between virtual sensor and measured values of indoor air temperature, indoor operative temperature and indoor relative humidity.

	Test Box West						Test Box East					
	T-air [K]		T-op [K]		rel. Hum [%]		T-air [K]		T-op [K]		rel. Hum [%]	
	North	South	North	South	North	South	North	South	North	South	North	South
Maximum Absolute Error	1.4	1.9	2.0	2.0	4.0	5.4	1.5	1.2	1.1	1.0	4.1	5.5
Mean Absolute Error	0.4	0.4	0.4	0.5	0.8	1.4	0.3	0.3	0.5	0.6	1.0	1.6
Root Mean Squared Error	0.5	0.5	0.7	0.7	1.2	1.8	0.5	0.4	0.7	0.8	1.6	2.0

The curve for the operative indoor temperature is of course again very similar to that of the indoor air temperature. The results for the indoor relative humidity also fit the measured values very well. The advantages of the CFD model with species transport are clearly visible. It reproduces fluctuating humidity levels clearly better than the BES model.

Table 3 shows a statistical analysis of the above-described deviations for the calculated time series. Here the maximum absolute error, the mean absolute error and the root mean squared error are summarised for both test boxes, all compared values and two sensors (North and South, see also Fig. 5) of each test box.

The maximum absolute error of the indoor air temperature is 1.9 K in test box west and therefore slightly higher than the 1.5 K in test box east. Also, the mean absolute error and the root mean squared error are slightly higher. This trend is also reflected in the values of indoor operative temperature and indoor relative humidity. We were already able to see this in the discussion of the graphs above. The root mean squared error weights the outliers more heavily and therefore shows slightly higher numbers than the mean absolute error. But from the fact that the numbers of both statistical KPIs are not far from each other we can see that there are not too may outliers in the deviations.

In general, the numbers of the Mean Absolute Error show very satisfying results. Also, the maximum absolute errors of all values are still acceptable, with good results especially for the test box east. This shows that the coupled simulation model with virtual sensors is working very well and can already be integrated in the HVAC control of buildings in future research work.

On examining the validation outcomes, we can identify the main causes for the deviations between virtual sensors and measured values. The outdoor air temperature sensors are influenced by direct solar radiation. Thus, the too high sensor readings for the outdoor air temperature lead to subsequent errors in the simulation models. Furthermore, the wrong boundary condition assumption for the ventilation system causes additional deviations. Thus, it can be said that the general quality of the coupled simulation model is very satisfactory. The deviations that occurred in this analysis can be significantly reduced by appropriate system corrections in future research work.

3.2. Simulation model runtime

By coupling the BES with the CFD model, simplifications can be made in the CFD model and thus the calculation time can be noticeably reduced. In previous CFD models, it was necessary to consider not only the air space but also all solid components as zones to be able to correctly simulate all transient heating and cooling processes [40,42]. The calculation of the transient processes was therefore always associated with long calculation times. Several hours were needed to simulate the transient thermal behaviour for a room zone of the size considered in this project. Depending on the size of the model or the number of grid cells, up to 20 h on a computer with an Intel Pentium i7 core processor with 6 physical cores were needed. Through the coupling, all transient thermal processes in the solid components are outsourced to the BES and no longer must be considered in the CFD simulation. As a result, only the room air zone remains as the single calculation volume and the calculation runtime of the CFD model can be significantly reduced to about 5–8 min, depending on the number of cells. The simulation runtime of the BES model lies at under 1 min. The total runtime of the coupled simulation model is thus less than 10 min. It follows that only the coupling between CFD and BES model shown here allows a simulation in real time with a conventional, state-of-the-art PC. This enables the newly developed virtual sensors to be integrated into the control of ventilation and air-conditioning systems of buildings.

3.3. Discussion and limitations

These results show a satisfactory model quality of the digital twin. The simulation runtime for one timestep can be reduced from around 20 h [40] to less than 10 min. Compared to that, the time step of the test buildings HVAC system lies at 15 min and therefore, the real-time requirement is fulfilled. At the same time, amongst other results, the average accuracy of the simulation over 5 consecutive days for all four virtual sensors lies at a mean absolute error of 0.35 K for the room air temperature and at 1.2% for the relative humidity. These outcomes demonstrate that this design of virtual sensors solve the trade-off problem between accuracy and computation time of model-based virtual sensors when applied in CFD models [5,7,24]. According to Refs. [27,28] this is fast and accurate enough to be implemented into the control of HVAC systems and thus to improve the indoor comfort and efficiency of buildings.

Nevertheless, we can also see two main points for further improvement in the results of the coupled simulation. Firstly, the quality of the sensor readings is highly dependent on the sensor positioning. In our case, the outdoor air temperature sensor was influenced by direct solar radiation. And secondly, the information about the ventilation systems volume flow and switching times gathered from a previous research project was wrong. The boundary conditions for the simulation were thus not set correctly. These input errors led to subsequent errors in the simulation models. From this we conclude that the used sensors and input variables should always be checked single-handedly for correctness and quality. Also, the assumed fraction of direct to diffusive solar radiation is a relatively rough estimate and caused deviations in the simulation results. Although the deviations were acceptable more detailed information about the solar radiation and its components would improve the output. An ordinary and in many cases freely available data feed from a nearby professional weather station, such as we used to double-check our sensors, would already be sufficient for this.

4. Conclusion

The aim of this research work was to develop a novel coupled simulation workflow for a digital twin with real-time, high accuracy virtual sensors. We can state that the virtual sensors are sufficiently fast and accurate to be implemented in the HVAC control of the test buildings used in the study.

One simulation run of the BES model lasts less than 1 min and one run of the most complex CFD model less than 8 min. This results

in a maximum simulation duration of under 10 min. This includes collecting data from the measurement system, starting the various simulation models and processing all the data using Matlab scripts. Compared to that, the time step of the test buildings HVAC system lies at 15 min. Therefore, the real-time requirement for the virtual sensors is fulfilled. In the validation with the measurement data of the test buildings the simulation results showed satisfying quality. The results of the virtual sensors over 5 consecutive days lie at a mean absolute error of 0.35 K for the room air temperature and at 1.2% for the relative humidity. Furthermore, the study showed the advantages of the CFD model in situations with more complex flow situations characterized by high fluid fluctuations.

The study showed that the digital twin and its virtual sensors are suitable to be implemented in the real-time control of HVAC systems. Additionally, we can state that the coupling workflow as it is designed can be adapted to any other indoor space of buildings.

The feedback of the virtual sensor data into the control of the test boxes was tested in a first trial, but the development of the complete control loop is the subject of future research. Therefore, the communication between the MS and DMS needs to be further improved and standardised. Also, the HVAC control must be adapted for a feed-in of the virtual sensor data.

In summary, we can state that the developed coupled simulation workflow performs very well and the novel digital twin with its virtual sensors can provide the desired data in real time and high accuracy. This enables the reproduction of the detailed thermal behaviour on a virtual level that is accurate and fast enough to be implemented into the control of air conditioning systems and will thus improve the comfort and efficiency of buildings.

Author statement

H.Edtmayer: Writing - Original draft, Writing - Review & Editing, Validation, Formal analysis, Visualisation.
D. Brandl: Conceptualization, Methodology, Software, Visualisation, Formal analysis, Investigation.
T. Mach: Conceptualization, Writing - Review & Editing, Supervision, Project administration, Funding acquisition, Resources.
E. Schlager: Software, Data Curation.
H. Gursch: Conceptualization, Resources, Writing - Original draft, Writing - Review & Editing, Project administration, Funding acquisition.
M. Lugmair: Conceptualization, Formal analysis.
C. Hochenauer: Writing - Review & Editing, Supervision.

Declaration of competing interest

The authors declare that they have no known competing financial interests or personal relationships that could have appeared to influence the work reported in this paper.

Data availability

The data that has been used is confidential.

Acknowledgements

This work is part of the project “COMFORT - Comfort Orientated and Management Focused Operation of Room condiTions” (No. 867533) funded by the program ‘ICT of the Future’ (6th Call 2017) of the Austrian Research Promotion Agency (FFG) and the Austrian Ministry for Transport, Innovation and Technology (BMVIT).

The Know-Center is funded within the Austrian COMET Program—Competence Centers for Excellent Technologies—under the auspices of the Austrian Federal Ministry of Transport, Innovation and Technology, the Austrian Federal Ministry of Economy, Family and Youth and by the State of Styria. COMET is managed by the Austrian Research Promotion Agency FFG.

References

[1] D. Enescu, A review of thermal comfort models and indicators for indoor environments, Renew. Sustain. Energy Rev. 79 (2017) 1353–1379, https://doi.org/10.1016/j.rser.2017.05.175.
[2] G. Halhoul Merabet, M. Essaaidi, M. Ben Haddou, B. Qolomany, J. Qadir, M. Anan, A. Al-Fuqaha, M.R. Abid, D. Benhaddou, Intelligent building control systems for thermal comfort and energy-efficiency: a systematic review of artificial intelligence-assisted techniques, Renew. Sustain. Energy Rev. 144 (2021), https://doi.org/10.1016/j.rser.2021.110969.
[3] T. Parkinson, A. Parkinson, R. de Dear, Continuous IEQ monitoring system: performance specifications and thermal comfort classification, Build. Environ. 149 (2019) 241–252, https://doi.org/10.1016/j.buildenv.2018.12.016.
[4] H.Y. Teh, A.W. Kempa-Liehr, K.I.-K. Wang, Sensor data quality: a systematic review, J. Big Data. 7 (2020), https://doi.org/10.1186/s40537-020-0285-1.
[5] D. Martin, N. Kühl, G. Satzger, Virtual sensors, Bus. \& Inf. Syst. Eng. 63 (2021) 315–323, https://doi.org/10.1007/s12599-021-00689-w.
[6] L. Fortuna, S. Graziani, A. Rizzo, M.G. Xibilia, Soft Sensors for Monitoring and Control of Industrial Processes, Springer, London, UK, 2007, https://doi.org/10.1007/978-1-84628-480-9.
[7] C.H. Guzmán, J.L. Carrera, H.A. Durán, J. Berumen, A.A. Ortiz, O.A. Guirette, A. Arroyo, J.A. Brizuela, F. Gómez, A. Blanco, H.R. Azcaray, M. Hernández, Implementation of virtual sensors for monitoring temperature in greenhouses using CFD and control, Sensors 19 (2019), https://doi.org/10.3390/s19010060.
[8] S.H. Khajavi, N.H. Motlagh, A. Jaribion, L.C. Werner, J. Holmström, Digital twin: vision, benefits, boundaries, and creation for buildings, IEEE Access 7 (2019) 147406–147419, https://doi.org/10.1109/ACCESS.2019.2946515.
[9] D.-G.J. Opoku, S. Perera, R. Osei-Kyei, M. Rashidi, Digital twin application in the construction industry: a literature review, J. Build. Eng. 40 (2021), https://doi.org/10.1016/j.jobe.2021.102726.
[10] S. Agostinelli, F. Cumo, G. Guidi, C. Tomazzoli, Cyber-physical systems improving building energy management: digital twin and artificial intelligence, Energies 14 (2021), https://doi.org/10.3390/en14082338.

[11] Y. Pan, L. Zhang, A BIM-data mining integrated digital twin framework for advanced project management, Autom. Constr. 124 (2021), https://doi.org/10.1016/j.autcon.2021.103564.
[12] L.C. Tagliabue, F.R. Cecconi, S. Maltese, S. Rinaldi, A.L.C. Ciribini, A. Flammini, Leveraging digital twin for sustainability assessment of an educational building, Sustain 13 (2021) 1–16, https://doi.org/10.3390/su13020480.
[13] G. Schrotter, C. Hürzeler, The digital twin of the city of zurich for urban planning, J. Photogramm. Remote Sens. Geoinf. Sci. 88 (2020) 99–112, https://doi.org/10.1007/s41064-020-00092-2.
[14] C. Vering, P. Mehrfeld, M. Nürenberg, D. Coakley, M. Lauster, D. Müller, Unlocking potentials of building energy systems' operational efficiency: application of digital twin design for HVAC systems, in: V. Corrado, E. Fabrizio, A. Gasparella, F. Patuzzi (Eds.), Build. Simul. Conf. Proc., International Building Performance Simulation Association (IBPSA), 2019, pp. 1304–1310, https://doi.org/10.26868/25222708.2019.210257.
[15] A. Zaballos, A. Briones, A. Massa, P. Centelles, V. Caballero, A smart campus' digital twin for sustainable comfort monitoring, Sustainability 12 (2020), https://doi.org/10.3390/su12219196.
[16] J. Ploennigs, A. Ahmed, B. Hensel, P. Stack, K. Menzel, Virtual sensors for estimation of energy consumption and thermal comfort in buildings with underfloor heating, Adv. Eng. Informatics. 25 (2011) 688–698, https://doi.org/10.1016/j.aei.2011.07.004.
[17] F. Ran, D. Gao, X. Zhang, S. Chen, A virtual sensor based self-adjusting control for HVAC fast demand response in commercial buildings towards smart grid applications, Appl. Energy. 269 (2020), https://doi.org/10.1016/j.apenergy.2020.115103.
[18] S. Alonso, A. Morán, D. Pérez, M.A. Prada, I. Díaz, M. Domínguez, Estimating cooling production and monitoring efficiency in chillers using a soft sensor, Neural Comput. Appl. 32 (2020) 17291–17308, https://doi.org/10.1007/s00521-020-05165-2.
[19] K. Liu, T.-Z. Liu, P. Fang, Z.-P. Li, Comprehensive approach to modeling and simulation of dynamic soft-sensing design for real-time building energy consumption, Int. J. Distrib. Sens. Networks. 13 (2017), https://doi.org/10.1177/1550147717704933.
[20] A. Gálvez, D. Seneviratne, D. Galar, Hybrid model development for HVAC system in transportation, Technologies 9 (2021), https://doi.org/10.3390/technologies9010018.
[21] I.P. Mohottige, T. Moors, Estimating room occupancy in a smart campus using WiFi soft sensors, in: IEEE 43rd Conf. Local Comput. Networks (LCN 2018), IEEE, New York, NY, USA, 2018, pp. 191–199, https://doi.org/10.1109/LCN.2018.8638098.
[22] L.V. Thanayankizil, S.K. Ghai, D. Chakraborty, D.P. Seetharam, Softgreen: towards energy management of green office buildings with soft sensors, in: Fourth Int. Conf. Commun. Syst. Networks (COMSNETS 2012), IEEE, New York, NY, USA, 2012, pp. 1–6, https://doi.org/10.1109/COMSNETS.2012.6151374.
[23] Y. Zhao, W. Zeiler, G. Boxem, T. Labeodan, Virtual occupancy sensors for real-time occupancy information in buildings, build, Environ 93 (2015) 9–20, https://doi.org/10.1016/j.buildenv.2015.06.019.
[24] W. Tian, X. Han, W. Zuo, M.D. Sohn, Building energy simulation coupled with CFD for indoor environment: a critical review and recent applications, Energy Build 165 (2018) 184–199, https://doi.org/10.1016/J.ENBUILD.2018.01.046.
[25] M. Barbason, S. Reiter, Coupling building energy simulation and computational fluid dynamics: application to a two-storey house in a temperate climate, Build. Environ. 75 (2014) 30–39, https://doi.org/10.1016/J.BUILDENV.2014.01.012.
[26] Y. Fan, K. Ito, Energy consumption analysis intended for real office space with energy recovery ventilator by integrating BES and CFD approaches, Build. Environ. 52 (2012) 57–67, https://doi.org/10.1016/J.BUILDENV.2011.12.008.
[27] P.H. Shaikh, N.B.M. Nor, P. Nallagownden, I. Elamvazuthi, T. Ibrahim, A review on optimized control systems for building energy and comfort management of smart sustainable buildings, Renew. Sustain. Energy Rev. 34 (2014) 409–429, https://doi.org/10.1016/J.RSER.2014.03.027.
[28] Z. Du, P. Xu, X. Jin, Q. Liu, Temperature sensor placement optimization for VAV control using CFD–BES co-simulation strategy, Build. Environ. 85 (2015) 104–113, https://doi.org/10.1016/J.BUILDENV.2014.11.033.
[29] P. Mehrfeld, M. Nürenberg, M. Knorr, L. Schinke, M. Beyer, M. Grimm, M. Lauster, D. Müller, J. Seifert, K. Stergiaropoulos, Dynamic evaluations of heat pump and micro combined heat and power systems using the hardware-in-the-loop approach, J. Build. Eng. 28 (2020), 101032, https://doi.org/10.1016/J.JOBE.2019.101032.
[30] S. Huang, W. Wang, M.R. Brambley, S. Goyal, W. Zuo, An agent-based hardware-in-the-loop simulation framework for building controls, Energy Build 181 (2018) 26–37, https://doi.org/10.1016/J.ENBUILD.2018.09.038.
[31] P.O. Fanger, Thermal Comfort: Analysis and Applications in Environmental Engineering, McGraw-Hill, 1972.
[32] M. Pichler, G. Görtler, H. Schranzhofer, H. Rieder, M. Herzlieb, N. Maierhofer, F. Wölfelmaier, M. Schneidhofer, Model Predictive Control von aktiven Bauteilen und Messungen in zwei Test-BOXen, Technical report, Proj. Im Rahmen Des Program, Haus Der Zukunft plus - Entwurf, 2017.
[33] M.F. Pichler, G. Goertler, H. Schranzhofer, Test buildings with TABS for MPC-performance evaluation-Comparability and system identification, 2016, Eur. Control Conf. ECC 2016 (2017) 1177–1182, https://doi.org/10.1109/ECC.2016.7810449.
[34] T. Mach, A. Heinz, D. Brandl, T. Schlager, M. Rennhofer, T. Selke, H. Gartner, M. Hinteregger, G. Zotter, G. Reinberger, J. Reckenzaun, M. Grobbauer, S. Grabmaier, M. Muller, COOLSKIN - Autarkes Kuhlen uber Gebaudehullen, (2019). https://energieforschung.at/projekt/autarkes-kuehlen-ueber-gebaeudehuellen/.
[35] T. Bröthaler, M. Rennhofer, D. Brandl, T. Mach, A. Heinz, G. Újvári, H.C. Lichtenegger, H. Rennhofer, Performance analysis of a facade-integrated photovoltaic powered cooling system, Sustain. 2021 13 (2021) 4374, https://doi.org/10.3390/SU13084374.
[36] A.B. Equa Simulation, IDA ICE Getting Started. Vol. Manual Version: 4.8, EQUA Simulation AB, Solona, Sweden, 2018.
[37] ANSYS, ANSYS Fluent User's Guide, Release 19, ANSYS, Inc., 2018. http://www.ansys.com.
[38] D. Brandl, T. Mach, M. Grobbauer, U. Ruisinger, C. Hochenauer, D. Brandl, T. Mach, M. Grobbauer, U. Ruisinger, C. Hochenauer, Analysis of natural convection and heat transfer for traditional box type windows, Int. J. Energy Convers. 1 (2013) 278–287, https://doi.org/10.15866/IRECON.V1I6.1431.
[39] D. Brandl, T. Mach, C. Hochenauer, Analysis of the transient thermal behaviour of a solar honeycomb (SHC) façade element with and without integrated PV cells, Sol. Energy. 123 (2016) 1–16, https://doi.org/10.1016/J.SOLENER.2015.11.004.
[40] D. Brandl, T. Mach, R. Heimrath, H. Edtmayer, C. Hochenauer, Thermal evaluation of a component heating system for a monastery cell with measurements and CFD simulations, J. Build. Eng. 39 (2021), 102264, https://doi.org/10.1016/j.jobe.2021.102264.
[41] Austrian meterological and geophysical service ZAMG, TAWES-Verlaufsgraphiken Graz Universität (2022) n.d, https://www.zamg.ac.at/cms/de/wetter/wetterwerte-analysen/tawes-verlaufsgraphiken/graz_universitaet/temperatur/?mode=geo&druckang=red. (Accessed 28 February 2022).
[42] P. Nageler, G. Schweiger, M. Pichler, D. Brandl, T. Mach, R. Heimrath, H. Schranzhofer, C. Hochenauer, Validation of dynamic building energy simulation tools based on a real test-box with thermally activated building systems (TABS), Energy Build 168 (2018) 42–55, https://doi.org/10.1016/J.ENBUILD.2018.03.025.